A Model-Based Feedforward Hysteresis Compensator for Micropositioning Control

Omar ALJANAIDEH [1] Micky RAKOTONDRABE [2], Isam AL-DARABSAH[3], and Mohammad AL JANAIDEH [4]

***Abstract*— Further results on a model-based hysteresis compensator that is constructed using inverse multiplicative structure of the Prandtl-Ishlinskii model are presented. This compensator can be used as a feedforward controller to compensate for the hysteresis nonlinearities of smart materials-based actuators at micro-scale level without employing the inverse model and feedback. The study presents the convergence analysis, compensation error, and parameters uncertainties for the proposed model-based hysteresis compensator. The results illustrate that considering low sampling time is essential to enhance the tracking performance in real-time system. The sampling time is calculated based on the Prandtl-Ishlinskii model parameters itself. The effectiveness of the proposed compensator was examined through numerical examples and in real-time system to a piezoelectric cantilever beam. A closed-loop controller was also applied with proposed compensator to verify the effectiveness of the proposed compensator. The experimental results show that the proposed model-based hysteresis compensator can be applied to compensate for hysteresis nonlinearities in micro positioning control systems.**

I. INTRODUCTION

Designing high precision positioning systems and micro- and nano-positioning applications such as observing and manipulating objects at micro and nano scale levels require employing smart material-based actuators that are able to provide fine resolution and fast response when imposed to external inputs such as voltage, current and temperature [1]–[3]. The benefits of these actuators come at a cost of hysteresis nonlinearities that are associated with oscillations in the open-loop system's responses, poor tracking performance and potential instabilities in the closed-loop system [4]. Consequently, several control algorithms have been suggested to cancel out the hysteretic effects of smart material-based actuators, these include adaptive control [5], energy-based control [6], robust control [7], [8], and inverse hysteresis models [4]. The Prandtl-Ishlinskii model is considered one of the most popular models that have been used with its inverse model for modeling and compensation of hysteresis of smart material-based actuators [3], [4], [9].

The Prandtl-Ishlinskii model, in particular, is considered attractive for modeling and compensation of hysteresis nonlinearities due to its suitability and simplicity for real-time applications [11]. The classical version of this model has been extended in [12] to a rate-dependent version. The rate-dependent Prandtl-Ishlinskii (RDPI) model can describe the hysteretic behaviour of smart material-based actuators which incorporates rate-independent hysteresis at shallow levels of excitation frequency, as well as rate-dependent hysteresis nonlinearities at high excitation frequencies [10].

Recently [11], a new methodology that considers restructuring the model itself in an inverse multiplicative scheme has been suggested for compensation of hysteresis nonlinearities of smart actuators. The inverse multiplicative scheme has been successfully applied to reduce the hysteresis nonlinearities characterized by the classical Bouc-Wen model [13] and the Prandtl-Ishlinskii model [11] which has been extended in [14], [15] for the RDPI model. Although this methodology can effectively compensate for the rate-dependent hysteresis without formulating rate-dependent inverse model as in [14], the convergence analysis of the error which is essential for applying feedback control algorithms has not been investigated. Synthesizing feedback control methodologies such as robust control and internal model based feedback control to improve the performance of a plant that exhibit dynamic hysteresis nonlinearities necessitates adequate consideration for the convergence analysis of the error when the inverse multiplicative scheme is applied.

In this paper, the convergence analysis of the error when the inverse multiplicative structure of the RDPI model is applied as a compensator is presented. This analysis aims at facilitating the implementation of the feedback control algorithms in order to improve the performance of hysteretic dynamic plant that is associated with parameters uncertainties.

II. REVISITING THE RATE-DEPENDENT PRANDTL-ISHLINSKII MODEL

The proposed compensator is a model-based controller constructed using the rate-dependent Prandtl-Ishlinskii model. In this section, we remind the rate-dependent Prandtl-Ishlinskii (RDPI) model which is often used for model implementation or for real-time compensation. The model is presented in this section along with the corresponding discrete form. The rate-dependent Prandtl-Ishlinskii (RDPI) model [12] has been recently suggested to describe the

[1] O. ALJANAIDEH was a research associate at the Department of Automatic Control and Micro-Mechatronic Systems, FEMTO-ST, AS2M, Univ. Bourgogne Franche-Comté, Univ. de Franche-Comt/CNRS/ENSMM/UTBM, FEMTO-ST Institute, Besançon France. email: omaryanni@gmail.com

[2] M. RAKOTONDRABE is with the Department of Automatic Control and Micro-Mechatronic Systems, FEMTO-ST, AS2M, Univ. Bourgogne Franche-Comté, Univ. de Franche-Comt/CNRS/ENSMM/UTBM, FEMTO-ST Institute, Besançon France, email: mrakoton@femto-st.fr

[3] I. AL-DARABSAH Department of Mathematics and Statistics, Memorial University of Newfoundland, St. John's NL, A1C 5S7, Canada. email: isam.matter@gmail.com

[4] M. Al JANAIDEH is with the Department of Mechanical and Industrial Engineering, University of Toronto, Toronto, ON M5S 3G8, Canada, email: mohammad.aljanaideh@utoronto.ca

rate-dependent hysteresis loops between input (voltage or current) and the output displacement of piezoelectric and magnetostrictive actuators.

A. The model

The discrete RDPI model can be represented with the sampling time T_s, where $T_s = t_k - t_{k-1}$, $k = 1, 2, \ldots, K$, and $K \in \mathbb{N}$ is an integer. With the applied input $z(k)$ and the rate of the input $v(t)$, the output of the discrete RDPI model is

$$y(k) = \Gamma[z](k) := \rho_0 z(k) + \Omega[z](k)\,, \tag{1}$$

where$\Omega[z](k) = \sum_{i=1}^{n} \rho_i \Phi_{r_i(v(k))}[z](k)$ and the discrete RDP (rate-dependent play) operator $\xi_i(k) = \Phi_{r_i(v(k))}[z](k)$ and $\xi_i(k) = \max\{z(k) - r_i(v(k)),\ \min\{z(k) + r_i(v(k)),\ \xi_i(k-1)\}\}$, where $r_i(v(k)) = \delta_1 i + \delta_2 |v(k)|$.

B. Input-Output Monotonicity of the RDPI Model

In this section we consider input-output monotonicity between the input $z(k)$ and output $y(k)$ of the RDPI model. This is essential because the proposed compensator is constructed based on the RDPI model. For $k > 1$, (i)when the input $z(k)$ increases, we have $z(k) > z(k-1)$ and $\xi_i(k) > \xi_i(k-1)$, then the output of the model is $y(k) = \rho_0 z(k) + \sum_{i=1}^{n} \rho_i (z(k) - r_i(v(k)))$ and $y(k-1) = \rho_0 z(k-1) + \sum_{i=1}^{n} \rho_i (z(k-1) - r_i(v(k-1)))$. Let $\sigma_1(k) = z(k) - z(k-1)$ and $\sigma_2(k) = |v(k-1)| - |v(k)|$. Then

$$y(k) - y(k-1) = \sum_{i=0}^{n} \rho_i (\sigma_1(k) + \delta_2 \sigma_2(k)). \tag{2}$$

(ii) When the input $z(k)$ decreases, we have $z(k) < z(k-1)$ and $\xi_i(k) < \xi_i(k-1)$, then the output is expressed as $y(k) = \rho_0 z(k) + \sum_{i=1}^{n} \rho_i (z(k) + r_i(v(k)))$ and $y(k-1) = \rho_0 z(k-1) + \sum_{i=1}^{n} \rho_i (z(k-1) + r_i(v(k-1)))$. Then

$$y(k) - y(k-1) = \sum_{i=0}^{n} \rho_i (\sigma_1(k) + \delta_2 \sigma_2(k)). \tag{3}$$

Then we have $\sigma_2(k) = 0$ and (7) can be written as

$$y(k) - y(k-1) = \sigma(k) \sum_{i=0}^{n} \rho_i. \tag{4}$$

(iii) When the input $z(k)$ is not increasing or decreasing, we have $z(k) = z(k-1)$ and $\xi_i(k) = \xi_i(k-1)$. Then

$$y(k) = y(k-1). \tag{5}$$

Equation (4) shows the dependence of the output change on the weights $\sum_{i=0}^{n} \rho_i$ and sampling time T_s. Consequently, $\sum_{i=0}^{n} \rho_i$ and the dynamic thresholds $r_i(v(k))$ should be bounded and non-negative. The finite number of the RDP operators ensures that the slope at each point on the hysteresis loop is finite. It can be concluded that

$$y(k) - y(k-1) = \sum_{i=0}^{n} \rho_i (\sigma_1(k) + \chi(k) \delta_2 \sigma_2(k)) \tag{6}$$

where $\chi(k)$ is the signum function of $v(k)$. Considering $|v(k-1)| = |v(k)|$, then it can be concluded that

$$y(k) - y(k-1) = \sum_{i=0}^{n} \rho_i \sigma_1(k). \tag{7}$$

We conclude that the the RDPI model satisfies that input-output monotonicity. This analysis is presented to show the convergence analysis for the proposed compensator when used as a feedforward compensator.

III. An Inversion-Free Feedforward Rate-Dependent Compensator

A. The proposed compensator and the maximum compensation positioning

A new rate-dependent feedforward compensator, based on the inverse multiplicative scheme which only uses the RDPI model, is presented in this section for compensation of rate-dependent hysteresis nonlinearities without formulating an inverse model. The major advantage in the proposed methodology that there is no additional calculation required to obtain the compensator parameters. Thus, as long as the model is identified, the compensator is yielded. Furthermore, no condition should be satisfied in order to ensure the invertibility of the RDPI model. The output of the proposed compensator is

$$u(k) = \Pi[z](k) = \rho_0^{-1}\Big(z(k) - \Omega[u](k-1)\Big). \tag{8}$$

Introducing the proposed compensator as an input to the discrete RDPI model in (1), we have

$$y(k) = \Gamma\Big[\rho_0^{-1}\Big(z(k) - \Omega[u](k-1)\Big)\Big](k). \tag{9}$$

Let $\eta(k) = z(k) - \Omega[u](k-1)$. Then $y(k) = \rho_0\Big[\rho_0^{-1}\Big(\eta(k)\Big)\Big] + \Omega\Big[\rho_0^{-1}\Big(\eta(k)\Big)\Big]$ and

$$y(k) = z(k) + \Omega[u](k) - \Omega[u](k-1). \tag{10}$$

Then the error of compensation is $e(k) = \Omega[u](k) - \Omega[u](k-1)$, and

$$e(k) = \sum_{i=1}^{n} \rho_i \Big(\Phi_{r_i(v(k))}[u](k) - \Phi_{r_i(v(k-1))}[u](k-1)\Big). \tag{11}$$

To show the maximum compensation positioning error with the proposed compensator, we obtain

$$|e(k)| = |\Omega[u](k) - \Omega[u](k-1)|. \tag{12}$$

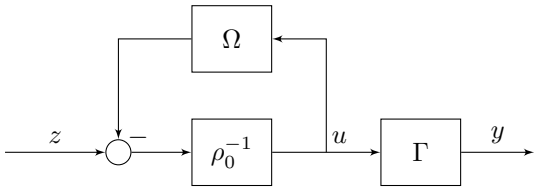

Fig. 1: The proposed compensator with the Prandtl-Ishlinskii hysteresis.

(i)When the input $u(k)$ increases, $u(k) > u(k-1)$, and for $A, B, C, D \in \mathbb{R}$, we have [18]

$$|\max\{A,B\} - \max\{C,D\}| \leq |\max\{|A-C|, |B-D|\}. \tag{13}$$

Then

$$|e(k)| \leq \sum_{i=1}^{n} \rho_i \max\{|u(k) - u(k-1) + r_i(v(k)) - r_i(v(k-1))|, |\xi_i(k) - \xi_i(k-1)|\}, \tag{14}$$

and $r_i(v(k)) - r_i(v(k-1)) = \delta_2(|v(k)| - |v(k-1)|)$. Let $u(k) - u(k-1) = \epsilon_u(k)$, $|v(k)| - |v(k-1)| = \epsilon_v(k)$, and $|\xi_i(k) - \xi_i(k-1)| = \epsilon_{\xi i}(k)$, then

$$|e(k)| \leq \sum_{i=1}^{n} \rho_i \max\{|\epsilon_u(k)| + \delta_2|\epsilon_v(k)|, |\epsilon_{\xi i}|(k)\}, \tag{15}$$

Let $\max|\epsilon_u(k)| = \epsilon_1$, $\max|\epsilon_v| = \epsilon_2$, and $\max|\ |\epsilon_{\xi i}|(k) = \epsilon_{3i}(k)$, where ϵ_1, ϵ_2, and ϵ_{3i} are small positive constants, and $\rho_{\max} = \max\{\rho_i\}$. Let $\epsilon_3 = \max \epsilon_{3i}$. Then we conclude

$$|e(k)| \leq n\rho_{\max} \max\{\epsilon_1 + \delta_2\epsilon_2, \epsilon_3\}. \tag{16}$$

Let $\epsilon = \max\{\epsilon_1 + \delta_2\epsilon_2, \epsilon_3\}$, then $|e(k)| \leq n\rho_{\max}\epsilon$. The error bound is $\mathcal{E} = n\rho_{\max}\epsilon$. For very small ϵ, the proposed compensator yields $y(k) \cong z(k)$. (ii)When the input $u(k)$ decreases, $u(k) < u(k-1)$, we have $|\min\{A,B\}\text{-}\min\{C,D\}| = |\max\{-C,-D\} - \max\{-A,-B\}|$, and

$$|\max\{-C,-D\} - \max\{-A,-B\}| \leq |\max\{|A-C|, |B-D|\}. \tag{17}$$

Then, we conclude that the error bound is $\mathcal{E} = n\rho_{\max}\epsilon$ and for very small ϵ, $y(k) \cong z(k)$(iii) For non-decreasing or non-increasing input $u(k)$, $u(k) = u(k-1)$, we have $\Omega[u](k) = \Omega[u](k-1)$ and the error $e(k) = 0$. Then we conclude$y(k) = z(k)$.

For the cases (i), (ii), and (iii) with the proposed compensator, it can be concluded that

$$\Gamma \circ \Pi[z](k) \cong z(k). \tag{18}$$

Thus, the proposed rate-dependent compensator ensures the tracking performance when the system typifies rate-dependent hysteresis nonlinearities.

B. Convergence analysis

In this section we study the convergence analysis for the proposed control method. For $k > 0$, we consider $\Delta e(k) = e(k) - e(k-1)$, then

$$\Delta e(k) = y(k) - y(k-1) - \{z(k) - z(k-1)\} \tag{19}$$

and

$$\Delta e(k) = \Omega(k) - 2\Omega(k-1) + \Omega(k-2))\}. \tag{20}$$

Then (i)when $u(k) > u(k-1)$, we have $\Delta e(k) = \sum_{i=1}^{n} \rho_i\big(\Delta\epsilon_u(k) - \Delta\epsilon_v(k)\big)$. Then

$$\Delta e(k) \leq \sum_{i=1}^{n} \rho_i|\big(\Delta\epsilon_u(k) - \Delta\epsilon_v(k)\big)|. \tag{21}$$

and

$$\Delta e(k) \leq n\rho_{\max}|\big(\Delta\epsilon_u(k) - \Delta\epsilon_v(k)\big)|. \tag{22}$$

(ii)When $u(k) < u(k-1)$, we have $\Delta e(k) = \sum_{i=1}^{n} \rho_i\big(\Delta\epsilon_u(k) + \Delta\epsilon_v(k)\big)$. Then

$$\Delta e(k) \leq n\rho_{\max}|\big(\Delta\epsilon_u(k) + \Delta\epsilon_v(k)\big)|. \tag{23}$$

(iii) When $u(k) = u(k-1)$, we have $\Delta e(k) = 0$. Then we conclude if $\Delta\epsilon_u(k) = \Delta\epsilon_v(k) = 0$, then

$$\Delta e(k) = 0. \tag{24}$$

Figure 1 displays the block diagram of the suggested methodology which shows that the scheme of the hysteresis compensator is a restructuration of the initial RDPI model using an inverse multiplicative scheme. The rate-dependent compensator is implemented in a feedforward open-loop manner for compensation of rate-dependent hysteresis nonlinearities. It should be noted that the delay block in the figure represents one sampling time T_s delay between the actual control input $u(k)$ and the one that used by the compensator.

IV. Compensation of Hysteresis in Smart Micropositioning Actuators

The RDPI model has been used to characterize hysteresis in different smart micropositioning actuators, such as piezoceramic actuators and magnetostrictive actuators. As shown in the pervious section that this study introduces a model-based feedforward controller using the RDPI model. Then it is essential to show the capability of the proposed feedforward controller considering characterization errors. In this section, the parameters uncertainty of RDPI model with the proposed compensator are presented.

A. Parameters Uncertainties

The output of the estimated discrete RDPI model is

$$\hat{y}(k) = \hat{\Gamma}[u](k) := \hat{\rho}_0 u(k) + \hat{\Omega}[u](k)\,, \tag{25}$$

where $\hat{\rho}_0$ is a positive constant and

$$\hat{\Omega}[u](k) = \sum_{i=1}^{n} \hat{\rho}_i \Phi_{\hat{r}_i(v(k))}[u](k), \tag{26}$$

where $\hat{\rho}_i$ are positive constants. The proposed compensator constructed with the estimated RDPI model is

$$u(k) = \hat{\rho}_0^{-1}\Big(z(k) - \hat{\Omega}[u](k-1)\Big). \tag{27}$$

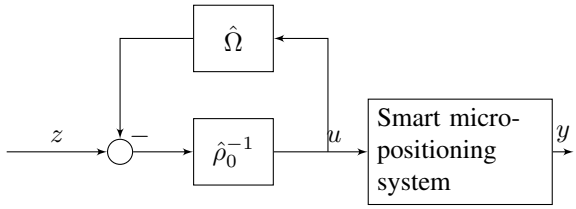

Fig. 2: The model-based feedforward compensator with a smart micropositioning system.

Then, the output of the compensation can be expressed as

$$y(k) = \rho_0 \hat{\rho_0}^{-1} z(k) - \rho_0 \hat{\rho_0}^{-1} \hat{\Omega}[u](k-1) + \Omega[u](k), \quad (28)$$

and the error is

$$e(k) = z(k)(1-\rho_0 \hat{\rho_0}^{-1}) + \rho_0 \hat{\rho_0}^{-1} \hat{\Omega}[u](k-1) - \Omega[u](k). \quad (29)$$

Let $\rho_0 \hat{\rho_0}^{-1} = \tau$ and $\mathcal{P}[k] = \rho_0 \hat{\rho_0}^{-1}\ \hat{\Omega}[u](k-1) - \Omega[u](k)$, then

$$\mathcal{P}[k] = \sum_{i=1}^{n} \left(\tau \hat{\rho}_i \Phi_{\hat{r}_i(v(k-1))}[u](k-1) - \rho_i \Phi_{r_i(v(k))}[u](k) \right). \quad (30)$$

and

$$\mathcal{P}[k] = \sum_{i=1}^{n} \max\{|\tau \hat{\rho}_i u(k-1) - \rho_i u(k) + \tau \hat{\rho}_i r_i(v(k-1)) - \rho_i r_i(v(k))|, |\xi_i(k) - \xi_i(k-1)|\}. \quad (31)$$

For $\hat{\rho}_i = \rho_i + \lambda_i$

$$\mathcal{P}[k] = \sum_{i=1}^{n} \max\{|(\tau\rho_i + \tau\lambda_i)u(k-1) - \rho_i u(k) + (\tau\rho_i + \tau\lambda_i) r_i(v(k-1)) - \rho_i r_i(v(k))|, |\xi_i(k) - \xi_i(k-1)|\} \quad (32)$$

and

$$|\mathcal{P}[k]| \leq \sum_{i=1}^{n} \max\{|\tau\rho_i u(k-1) - \rho_i u(k) + \tau\rho_i r_i(v(k-1)) - \rho_i r_i(v(k))| + \tau\lambda_i u(k-1) + \tau\lambda_i r_i(v(k-1)), |\xi_i(k) - \xi_i(k-1)|\} \quad (33)$$

Let $\max\{|\tau u(k) - u(k-1)|\} = \bar{\epsilon}_1$, $\max\{|u(k-1) + r_i(v(k-1)|\} = \kappa$, $\max|\tau r_i(v(k-1)) - r_i(v(k))| = \bar{\epsilon}_2$, and $\lambda_{\max} = \max\{|\lambda_i|\}$, where $\bar{\epsilon}_1$, $\bar{\epsilon}_2$, and κ are positive constants. Then the error is

$$|e(k)| \leq |z(k)||(1-\tau)| + n\rho_{\max}\{\bar{\epsilon}_1 + \bar{\epsilon}_2 + \lambda_{\max}\kappa, \epsilon_3\}. \quad (34)$$

We conclude that the tracking error is bounded when the uncertainties of the RDPI model parameters are considered for compensation of hysteresis nonlinearities. This can be obtained with very small sampling time. In this study we consider with the following equation to obtain the sampling time

$$T_s < \frac{1}{n(\rho_0 + 1)(\sum_{i=1}^{n} \rho_i + 1)(f_{\max} + 1)} \quad (35)$$

and considering

$$\rho_{\max} n < 1 \quad (36)$$

to reduce the error of the compensation with the proposed feedforward compensator.

B. Numerical example

Consider a reference input for a hysteretic positioning actuator is $z(k) = 20\sin(2\pi f k T_s)\ \mu m$ where $f = 1$, $f = 50$ and $f = 100$ Hz applied to a RDPI model formulated using $n = 5$ play operators and the parameters $\rho_0 = 0.6295$, $\rho_1 = 0.1617$, $\rho_2 = 0.1137$, $\rho_3 = 0.0611$, $\rho_4 = 0.0328$, $\rho_5 = 0.0716$, $\delta_1 = 1.7504$, and $\delta_2 = 3.7627 \times 10^{-4}$. The response of model under these excitations is presented in Figure 3 (a). The proposed compensator was subsequently applied at sampling time of 1×10^{-6} Sec to reduce the dynamic hysteresis loops of the RDPI hysteresis model considering $f_{max} = 500$. Figure 3 (b) shows the output of the RDPI model when the proposed compensator is applied in a feedforward manner at input excitations of 1, 50 and 100 Hz. Figure 3 (c) illustrates the time history of the error e and Δe when the proposed compensator is applied at input frequency of 50 Hz and sampling time of $T_s = 1 \times 10^{-6}$ Sec. The selected sampling time and weights satisfy both conditions (35) and (36).

The effectiveness of the proposed compensator was also explored at same excitation frequency $f = 50$ Hz but at sampling time of $T_s = 5 \times 10^{-4}$ Sec that violates condition (35). The time history of e and Δe are shown in Figure 3 (d), which illustrates that increasing the sampling time contributes substantial compensation errors. The compensation error signals e and Δe were also examined under 50 Hz excitation frequency at $T_s = 1 \times 10^{-6}$ Sec in Figure 3(e). The weights were selected to violate condition (36). As the figure demonstrates that ignoring condition (36) yields a dense noisy output signal that might effect the tracking performance os control systems in real-time system. The maximum error was finally explored as a function of the sampling time under input frequency of 50 Hz in Figure 3 (f). The figure shows that decreasing the sampling time contributes lower compensation error.

V. Application to a Piezoelectric Cantilevered Actuator

A. The experimental platform

In order to explore the effectiveness of applying the proposed rate-dependent compensator with the internal model-based feedback control, a piezoelectric cantilevered actuator was considered for experimental study. The proposed piezoelectric actuator exhibits the output displacement (deflection) $y[\mu m]$ when subjected to input voltage $u[V]$.

The piezoelectric cantilevered actuator was subjected to a sinusoidal harmonic input voltage of $8V$ amplitude at different excitations of frequency. Figure 4 shows the input voltage-output displacement rate-dependent hysteresis loops at $1Hz$, $90Hz$, $130Hz$ and $190Hz$ excitation frequency. As the figure illustrates, increasing the excitation frequency of the applied input yields a significant increase in the hysteresis nonlinearities of the actuator.

B. Open-loop compensation

The measured experimental results in Figure 4 were employed to identify the parameters of a RDPI model. The model was formulated on the basis of the discrete version presented in (1) and the two conditions (35) and (36). The identified RDPI model was then restructured to

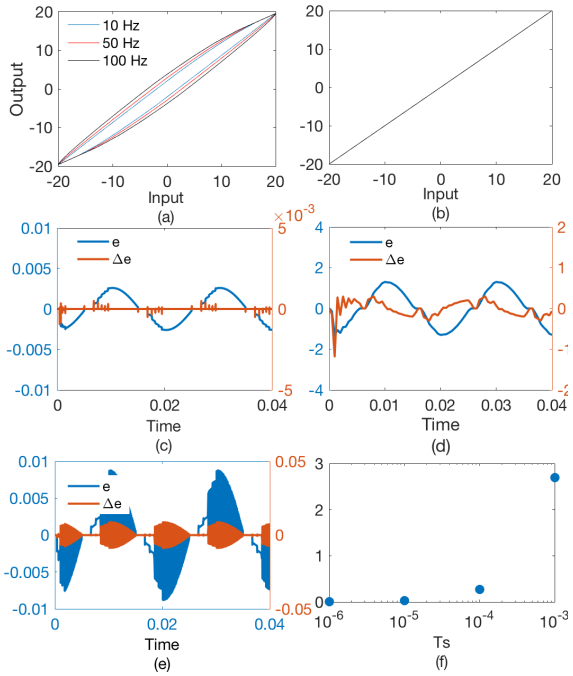

Fig. 3: (a) Input-output hysteresis of RDPI model at excitation frequency of 1, 50 and 100 Hz, (b) input-output of RDPI when the proposed compensator is applied at 1, 50 and 100 Hz, time-history of e and Δe at (c) 50 Hz excitation frequency and $T_s = 1 \times 10^{-6}$ Sec, (d) 50 Hz excitation frequency and $T_s = 5 \times 10^{-4}$ Sec, (e) 50 Hz excitation frequency and $T_s = 1 \times 10^{-6}$ Sec while violating condition (36) and (f) the maximum error at different samplings of time.

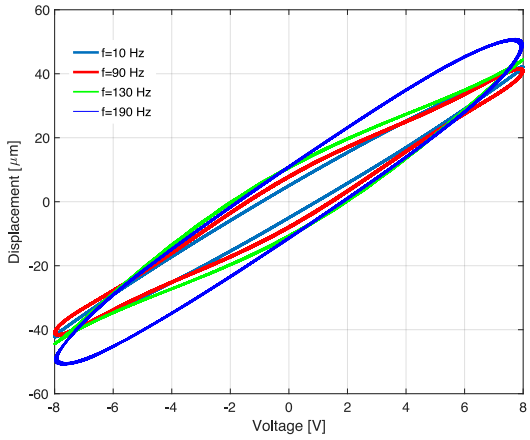

Fig. 4: Measured hysteresis loops at $8V$ amplitude applied at $1Hz$, $90Hz$, $130Hz$ and $190Hz$ excitation frequency.

obtain the corresponding inverse multiplicative scheme as illustrated in Figure 2 for compensation of rate-dependent hysteresis nonlinearities of the piezoelectric cantilevered actuator. The effectiveness of the proposed compensator was subsequently examined at different excitations of input frequency differ than those employed to identify the RDPI model. The output displacement of the actuator when the proposed rate-dependent compensator is applied as a feedforward compensator are given in Figure 5. The figure shows the desired output displacement $y_{[}\mu m]$ versus the resulting output displacement $y[\mu m]$ at different frequencies in the $0.1Hz$ - $220Hz$ range. The compensation results demonstrate that the suggested rate-dependent compensator can be employed to cancel out the rate-independent and rate-dependent hysteresis nonlinearities of the piezoelectric cantilevered actuator. However, at very higher excitations, the compensation results revealed slight error e that is mostly attributed to the other dynamics that could not be represented by the proposed RDPI model.

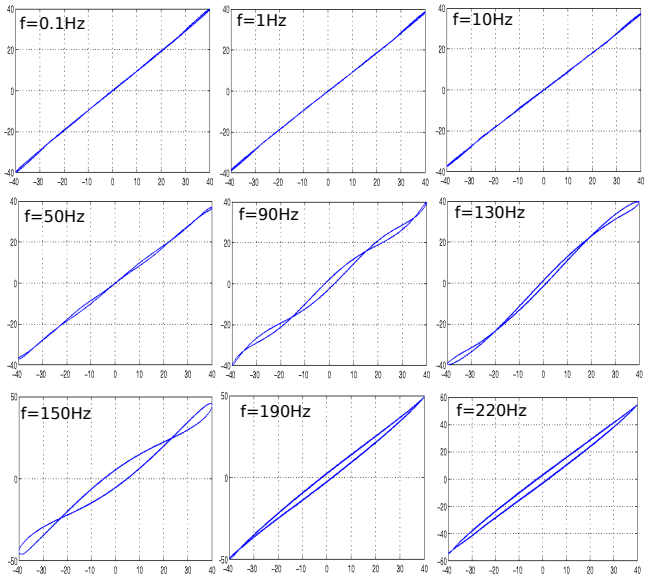

Fig. 5: The hysteresis loops of the piezoelectric cantilevered actuator when the proposed compensator is applied for compensation of hysteresis nonlinearities.

VI. Closed-loop compensation

The previous sections dealt with the feedforward compensation of the rate-dependent hysteresis of the initial system. The compensator was based on the combination of the RDPI model that captures the hysteresis and the inverse multiplicative structure. However, feedforward control is known to lose efficiency when there are internal or external perturbations acting to the system. The error $e(k)$ can be considered as an internal perturbation of a linear system. Thus, the system can be represented using a linear model subjected to a disturbance:

$$y(t) = G(s)y_r(s) + e(s) \tag{37}$$

where $G(s) = 1$, where y_r is the reference displacement input. Since there are always high dynamics that could not be represented by the RDPI and hence were not compensated then $G(s) \neq 1$. In the sequel, we leave $G(s)$ in order to consider such more general case. The identification of $G(s)$

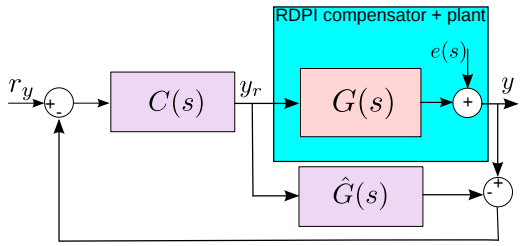

Fig. 6: Feedforward control augmented by an internal model feedback scheme.

can be done with the new system having as input y_r and output y, see Figure 1.

In this section, we augment the previous feedforward scheme with a feedback controller in order to add robustness and improve the tracking objective. The internal model scheme will be employed as a feedback control, which permits the consideration of the perturbation and modeling error in $G(s)$. Figure 6 shows the feedforward scheme augmented by the internal model based feedback control. In the figure, r_y is the exogeneous reference input, while $C(s)$ and $\hat{G}(s)$ represent the feedback controller to be calculated. In fact, the objective is to obtain a $\hat{G}(s)$ as equal as possible to the real behavior $G(s)$. $\hat{G}(s)$ is therefore an approximate model of $G(s)$. From Figure 6, we have

$$y = \frac{GC}{\left(1 + C\left(G - \hat{G}\right)\right)} r_y + \frac{\left(1 - \hat{G}C\right)}{\left(1 + C\left(G - \hat{G}\right)\right)} e \quad (38)$$

Selecting $C(s) = \frac{1}{\hat{G}(s)}$. Thus, $y = r_y + 0 \times e$, which implies that the steady-state error is always null and the disturbance is always rejected irrespective to the constant $e(t)$, constant reference $r_y(t)$ and any approximate model $\hat{G}(s)$. However, this choice only improves the steady-state regime and ignores transient part. In order to consider a transient part with a desired settling time t_r for the closed-loop, let us choose $C(s) = F(s)\frac{1}{\hat{G}(s)}$ where the filter $F(s) = \frac{1}{1+\frac{t_r}{3}s}$ directly corresponds to the desired closed-loop behavior. Notice that, in that case, if the internal model $\hat{G}(s)$ is exact ($\hat{G}(s) = G(s)$), we have: $y(s) = F(s)r_y(s) + (1 - F(s))\, e(s)$. Consequently, the desired transient part, the zero steady-state error and the disturbance rejection are guaranteed. However, if $\hat{G}(s)$ is not exact, we have $y = \frac{\frac{G}{\hat{G}}F}{\left(1+F\left(\frac{G}{\hat{G}}-1\right)\right)} r_y + \frac{(1-F)}{\left(1+F\left(\frac{G}{\hat{G}}-1\right)\right)} e$. In such case, the steady-state error is still zero and the disturbance still rejected. However, the transient part differs from the desired transient part $F(s)$. This difference increases with if $\hat{G}(s)$ has not been identified properly.

VII. Internal Model-Based Feedback Control Design

The convergence analysis in section III allows designing feedback controllers that can be applied with the proposed rate-dependent compensator to facilitate connecting smart actuators to dynamic plants so as to deliver the desired displacement without hysteresis nonlinearities. The dynamic model $\hat{G}(s)$ was identified from output displacement that was measured after applying a desired step input of $y_r = 40\mu m$ to the compensated system. The dynamic model $\hat{G}(s)$ was identified as:

$$\hat{G}(s) = \frac{-19.6(s-1.2e5)(s+3e4)(s-2.8e4)(s-1.1e4)(s+1430)}{(s^2+925s+4.6e5)(s^2+55s+1.4e7)(s^2+1.5e4s+4e9)} \frac{(s^2+4.3e4s+3.2e9)}{(s^2+965s+3.9e9)} \quad (39)$$

where $e\theta$ denotes $\times 10^{\theta}$, for instance $3e4 = 3 \times 10^4$. Figure 7 presents a comparison between both the experimental step response measured from the piezoelectric cantilevered actuator and the step response of the identified model $\hat{G}(s)$.

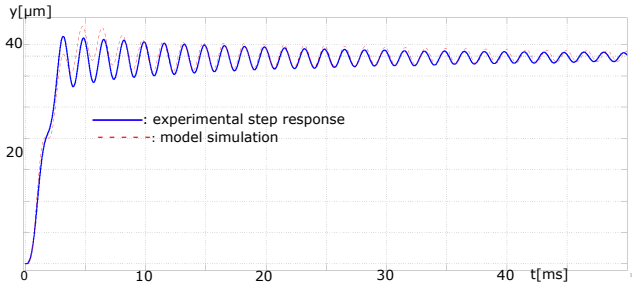

Fig. 7: A comparison between the step response of the piezoelectric cantilevered actuator and the identified linear model $\hat{G}(s)$.

After estimating the $\hat{G}(s)$ that can represent the real dynamic model $G(s)$ of the compensated system, a feedback behavior $F(s)$ has to be identified. A transient response without overshooting and with a settling time of $t_r = 20ms$ was considered as desired specifications for the closed-loop control design. These specifications were selected to obtain a better tracking compared to the response obtained from the initial system $\hat{G}(s)$ (and $G(s)$) in Figure 7. Constructing $F(s)$ based on desired requirements was employed to yield the controller $C(s)$ such that $C(s) = F(s)\frac{1}{\hat{G}(s)} = \frac{1}{(1+6.7\times10^{-3}s)\hat{G}(s)}$, where $\hat{G}(s)$ is given by (39). A step input $r_y = 40\mu m$ was applied to the closed-loop augmented system. The measured output displacement of the actuator when the reference input $r_y = 40\mu m$ is applied is shown in Figure 8 (a) the figure shows that the desired specifications are fully respected. The maximum error under a sinusoidal harmonic input $r_y(t) = 40\mu m \sin(2 \times \pi \times f \times t)$ was evaluated under different excitations of frequency in Figure 8 (b). As both figures illustrate, the desired specifications are fully respected and the proposed compensator can be employed with with feedback controllers to improve the tracking performance of piezoelectric cantilevered actuators.

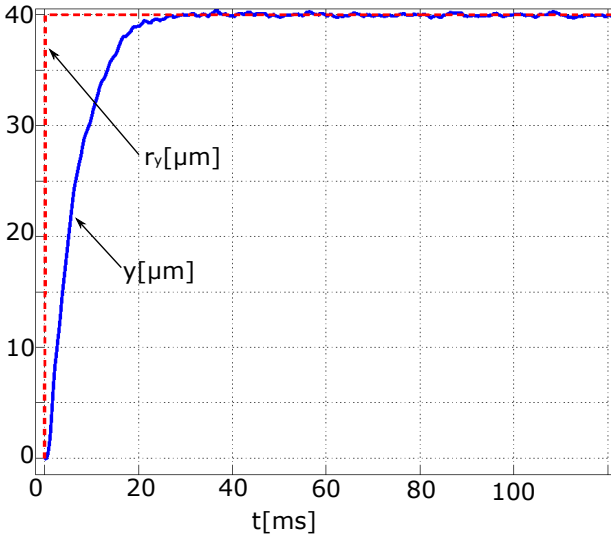

(a)

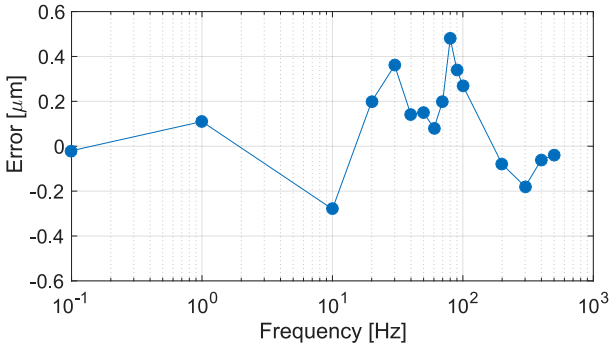

(b)

Fig. 8: (a) Experimental step response of the closed-loop with the proposed internal model controller, (b) Maximum positioning error with the proposed controller under sinusoidal harmonic input applied at different excitations of frequency.

VIII. Conclusions

This paper investigated the convergence analysis when the rate-dependent Prandtl-Ishlinskii hysteresis model (RDPI) combined with an inverse multiplicative structure are combined and used to compensate for rate-dependent hysteresis of smart material based actuators. The analysis demonstrated that the output of the compensated system is equivalent to a linear system followed by a bounded error. This formulation was afterwards used to construct a closed-loop feedback controller based on the internal model architecture. Both the feedforward and feedback control approaches were afterwards applied experimentally to a piezoelectric cantilevered actuator. The experimental results showed that the suggested compensation methodology can be employed with a feedback control architecture to improve the performance.

References

[1] R. Smith, *Smart material system: Model development*, SIAM, 2005.

[2] W. Nagel, G. Clayton, and K. Leang, "Master-slave control with hysteresis inversion for dual-stage nanopositioning systems," *Proceesings of American Control Conference*, Boston, MA, pp. 655-660, 2016.

[3] M. Rakotondrabe, *Smart materials-based actuators at the micro/nano-scale: characterization, control and applications,* Springer-Verlag, NewYork, 2013.

[4] C. Visone, "Hysteresis modelling and compensation for smart sensors and actuators," *Journal of Physics: Conference Series*, vol. 138, 2008.

[5] M. Al Janaideh and D. S. Bernstein, "Inversion-free adaptive control of uncertain systems with SMA actuation," *Proceedings of the American Control Conference*, pp. 3585-3590, Washington, DC, 2013.

[6] W. Oates, P. Evans, R. Smith, M. Dapino, "Experimental implementation of a hybrid nonlinear control design for magnetostrictive actuators", *Journal of Dynamic Systems, Measurement, and Control*, vol. 131, no. 4 041004, 2009.

[7] M. Rakotondrabe, Y. Haddab and P. Lutz, "Quadrilateral modelling and robust control of a nonlinear piezoelectric cantilever," *IEEE Transactions on Control Systems Technology*, vol.17, no. 3, pp. 528-539, 2009.

[8] M. Rakotondrabe, K. Rabenorosoa, J. Agnus, and N. Chaillet, "Robust feedforward-feedback control of a nonlinear and oscillating 2-dof piezocantilever," *IEEE Transactions on Automation Science and Engineering*, vol. 8, no. 3, pp. 506-519, 2011.

[9] X. Tan and J. S. Baras, "Modeling and control of hysteresis in magnetostrictive actuators," *Automatica*, vol. 40, no. 9, pp. 1469-1480, 2004.

[10] O. Aljanaideh, M. Al Janaideh, C-Y. Su, and S. Rakheja, "Compensation of rate-dependent hysteresis nonlinearities in a magnetostrictive actuator using an inverse Prandtl-Ishlinskii model," *Smart Materials and Structures*, vol. 22, no. 3, doi:10.1088/0964-1726/22/2/025027, 2013.

[11] M. Rakotondrabe, "Classical Prandtl-Ishlinskii modeling and inverse multiplicative structure to compensate hysteresis in piezoactuators," *Proceedings of the American Control Conference*, Montreal, Canada, pp. 1646-1651, 2012.

[12] M. Al Janaideh and P. Krejčí, "Inverse rate-dependent Prandtl-Ishlinskii model for feedforward compensation of hysteresis in a piezomicropositioning actuator," *IEEE/ASME Transactions on Mechatronics*, vol 18, no. 5, pp. 1498-1507, 2013.

[13] M. Rakotondrabe, "Bouc-Wen modeling and inverse multiplicative structure to compensate hysteresis nonlinearity in piezoelectric actuators," *IEEE Transactions on Automation Science and Engineering*, vol. 8, no. 2, pp. 428-431, 2011.

[14] O. Aljanaideh, M. Al Janaideh, and M. Rakotondrabe, "Inversion-free feed-forward dynamic compensation of hysteresis nonlinearities in smart Micro/Nano- positioning actuators," *Proceedings of the IEEE Conference on Robotics and Automation*, pp. 2673-2678, Seattle, WA, 2015.

[15] O. Aljanaideh, M. Rakotondrabe, H. Khasawneh, and M. Al Janaideh, "Rate-dependent Prandtl-Ishlinskii hysteresis compensation using inverse-multiplicative feedforward control in magnetostrictive Terfenol-D based actuators," *Proceedings of the American Control Conference*, pp. 649-654, Bosotn, MA, 2016.

[16] M. Al Janaideh and P. Krejci, "A Rheological model for the rate-dependent Prandtl-Ishlinskii model," *Proceedings of the 52nd IEEE Conference on Decision and Control*, pp. 6646-6651, Firenze, Italy, 2013.

[17] R. Burden and J. Faires, "*Numerical Analysis*," 7th Edition, Brooks/Cole, ISBN 0-534-38216-9, 2000.

[18] M. Brokate and J. Sprekels, *Hysteresis and Phase Transitions*, New York, NY, Springer, 1996.

[19] M. Edardar, X. Tan, and H. Khalil, "Design and analysis of sliding mode controller under approximate hysteresis compensation," *IEEE Transactions on Control Systems Technology*, vol. 23, no. 2, pp. 598 - 608, 2014.

[20] William S. Oates, R. Zrostlik, S. Eichhorn, R. Smith, "A Non-linear optimal control design using narrowband perturbation feedback for magnetostrictive actuators", *Journal of Intelligent Material Systems and Structures*, vol. 21, pp. 1681-1693, 2010.

[21] S. Yingfeng and K.K. Leang, "Design and control for high-speed nanopositioning: serial-kinematic nanopositioners and repetitive control for nanofabrication," *IEEE Control Systems Magazine*, vol. 33, no. 6, pp. 86-105, 2013.

[22] J. Agnus, N. Chaillet, C. Clvy, S. Dembl, M. Gauthier, Y. Haddab, G. Laurent, P. Lutz, N. Piat, K. Rabenorosoa, M. Rakotondrabe and B. Tamadazte, "Robotic Microassembly and micromanipulation at FEMTO-ST", Journal of Micro-Bio Robotics, vol. 8, no. 2, pp. 91-106, 2013.